

Fast Ion Loss Diagnostic in ASDEX Upgrade

M. Garcia-Munoz, H.-U. Fahrbach, J. Neuhauser, H. Zohm, A. Herrmann, V. Rohde and ASDEX Upgrade Team

Max-Planck-Institut für Plasmaphysik, EURATOM Association
Boltzmannstr. 2, D-85748 Garching b. München, Germany

Introduction

The confinement of fast particles is of crucial importance for next step fusion devices like ITER. Since fast ion losses might reduce the core heating and, in addition, cause intolerable first wall load, it is important to understand and possibly avoid them. Here, an integrated approach is presented for the analysis of neutral beam injection related fast ion losses in ASDEX Upgrade. It consists of a scintillator based fast ion detector mounted on the low field side mid plane manipulator, together with a code package [1] simulating particle trajectories from their birth places in the plasma out to the detector. Classical collisions as well as the effect of core and edge MHD activity and the toroidal magnetic field ripple on the fast ions are taken into account. In addition to these ion losses from the core, containing the desired physics information, ions generated in the edge region may hit the detector essentially without plasma interaction and hence with full injection energy ('prompt' or 'first orbit' losses). In experiment, these can be used for detector calibration.

In the following, a brief description of the diagnostic design is given followed by first measurements of prompt and MHD induced losses of fast ions. The effects of edge localized modes (ELMs), and classical and neo-classical tearing modes on the fast ion loss spectrum, observed for the first time in a fusion plasma device, are reported.

Experimental Set-Up

The new fast ion loss diagnostic (FILD) is mounted on the ASDEX Upgrade midplane manipulator. This allows one to vary, from discharge to discharge, the radial position of the detector head in order to find the most appropriate radial position for each phenomenon to be studied. The detector acts as a magnetic spectrometer, dispersing fast ions onto a scintillator, with the hit point depending on their gyroradius and pitch angle. The design is based on the concept of the α -particle detector used for the first time at TFTR [2] and more recently at W7-AS [3]. The detector head consists basically of an 3-dimensional ion collimator, a double stainless steel plate coated with the scintillator powder and a graphite cap. The geometry of the collimator has been optimized by simulating typical particle trajectories of interest using the GOURDON code. A schematic view of the detector principle is shown in figure 1. The gyroradius of the particle orbit determines how far from the aperture the particle will strike the scintillator. The pitch angle determines where the particle will strike along the orthogonal dimension of the scintillator. On the right hand side of the figure a poloidal cross section of ASDEX Upgrade is shown with the position of the probe on the manipulator just behind the

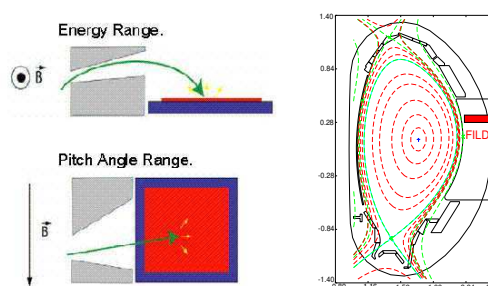


Figure 1: Detector principle and poloidal cross section of ASDEX Upgrade with manipulator behind ICRH antenna limiter.

antenna limiter. The final geometry chosen enables the detection of particles with energies up to 150 keV and pitch angles ($V_{\text{perp}}/V_{\text{tot}}$) between 0.99 (deeply trapped particles) and 0.4 (passing ions). The graphite cap shape was calculated by following the fast ions backwards in time from the aperture. The final shape was chosen to be the one that does not interfere with the fast ion trajectories. A novel scintillator has been used. Since it has a very fast decay time ($< 1\mu\text{s}$) compared with previous similar detectors, it allows one to observe very fast MHD phenomena on the lost ion population. The temperature of the graphite cap is measured to avoid possible undesirable overheating of the probe. The quantum efficiency of the scintillator depends on its temperature and this is no longer constant at temperatures above 400°C . The total particle flux to the isolated scintillator plate is determined by measuring the electric current to it. To exclude artefacts, the hidden second plate, not exposed to ions and isolated from the first one by a ceramic layer was used as a reference.

Using a lense relay and a beam splitter, the light pattern on the scintillator is then recorded with high spatial resolution by a CCD camera with a moderate frame rate between 25 and 100 Hz and, in parallel, through an optical fiber bundle, connecting a preselected array of fields on the scintillator to a set of photomultipliers. Their signals are sampled with up to 1 MHz and can be used to analyse very fast events at reduced spatial resolution.

Results: Fast Ion Losses in ASDEX Upgrade

I. Prompt Losses

In order to check the design of the detector head, its aperture and the resolution in phase space, the system was exposed to high fluxes of prompt losses with different energies and pitch angles. For this purpose, the box 2 of the ASDEX Upgrade neutral beam injector system was used, which is located toroidally only one sector apart from the probe. The four sources in the box all have different injection geometry and, accordingly, different patterns were observed as expected, when the sources were switched on sequentially.

With fixed injection energy, neutrals injected more radially result in ion loss spots with the correct energy and higher perpendicular velocity component, than those injected more tangentially. In fact, all sources can be clearly identified in FILD by their prompt loss pattern. In the following investigation of core related losses, only box 1, placed toroidally opposite to box 2, will be used to reduce the interference between the desired core loss signals (in principle related to box 1 or 2) and the much stronger prompt losses, which come mostly from box 2.

II. MHD induced fast ion losses

Effects of ELMs on fast particles

ELM induced fast ion losses have been directly observed for the first time in a fusion plasma device by this diagnostic. A very narrow optical filter for the wave length of the scintillator emission was used during a few discharges to eliminate the possibility that the detector was

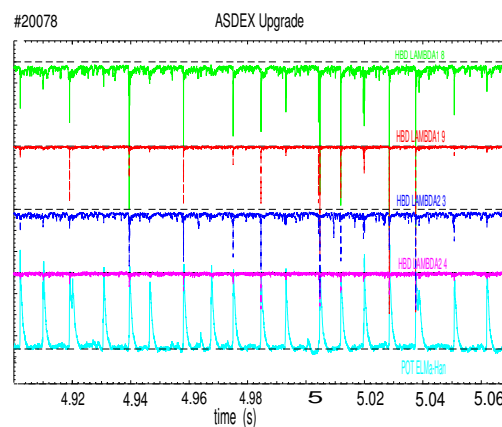


Figure 2: ELM induced fast ion losses measured by various fast detector channels compared with the D_α signal in the outer divertor (bottom).

measuring light coming from the plasma through the aperture. In figure 2, the time traces of different photomultipliers, representing different energy and pitch angle, are shown in comparison to the divertor D_α signal. Obviously, not every ELM produces the same spikes in phase space. This means that different ELMs eject particles with different energies and pitch angles, depending probably on their actual characteristics. Looking in more detail, one finds that a fraction of the fast ions is lost in a very short pulse immediately after the onset of the ELM turbulence seen by magnetic pick-up coils.

Depending on the ELM sub-structure, even several isolated spikes occur during one ELM. Such a case is shown in figure 3 where three multiplier signals are plotted for a single ELM together with the magnetic signal from a pick-up coil located on the same helical flux bundle, but several meters away toroidally. There are three fast ion pulses apparently correlated with sub-structures in the magnetic signal. The D_α signal in the divertor plotted in addition shows that the spikes occur only during the magnetic turbulence phase, essentially coincident with the D_α rise phase.

Whether the spectral change over the three spikes is just random or indicates a systematic trend during the ELM remains to be investigated. In parallel, investigation of heat loads to adjacent limiters and to the probe head using an infra-red camera [4] have revealed similar time behaviour of ELM induced energy losses, but without any assertion on their energy or pitch angle.

NTM induced fast ion losses

Enhanced fast ion losses were observed in specific spectral ranges in presence of resistive as well as neoclassical tearing modes (NTM). Results obtained during a (3,2) and a (2,1) NTM are presented here. During a (3,2) NTM phase, ions were detected with energies around 5 keV and pitch angles corresponding to deeply trapped orbits as can be seen in the CCD camera view shown in figure 4a. On the same picture a mesh for energy and pitch angles has been drawn together with matrix of the scintillator fields (indicated by numbers) observed by the fast photomultiplier system as described earlier. From the latter it is obvious that the ion loss signal is not continuous in time, but is clearly correlated with the ELM related magnetic turbulence just before and during the rise of the remote divertor D_α emission (figure 4b), as discussed in the previous section. Our interpretation is that the loss occurs in a two-step process with the NTM driving core ions towards the edge, from where they are discontinuously transported to the detector mostly by the transient magnetic turbulence.

Fast ions ejected by a (2,1) mode with higher energies (40-60 keV) and higher parallel component of the velocity were detected in a strongly puffed discharge with small high frequency ELMs. A corresponding CCD camera view is shown in figure 5a. The ELM induced magnetic turbulence was an order of magnitude smaller than with large type-I ELMs, and accordingly no correlation between FILD and ELM signatures was found. Instead, the losses were fully time correlated with the odd-n Mirnov coil signal as seen in figure 5b, indicating a fixed phase relation between the periodic mode signal and the particle flux. This could be due to an electric field induced by a difference in motion between mode and fluid [5].

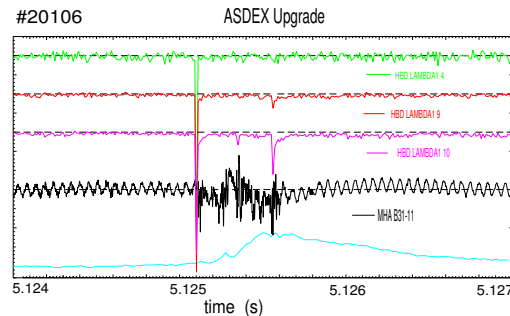


Figure 3: ELM ejecting different particles at different times. From top: 3 FILD channels, magnetic pick-up coil and D_α signal.

There is, however, still some uncertainty with respect to the fast ion spectrum, since the edge neutral density is raised by the intense gas puff to a level where charge exchange (CX) with deuterium molecules and atoms becomes an important loss channel for fast ions between the plasma edge and the detector. In effect, because of the strong drop of the CX cross section between 10 and 100 keV, the ion flux seen by the detector at lower energies could be significantly reduced, while the highest energies might be nearly unaffected.

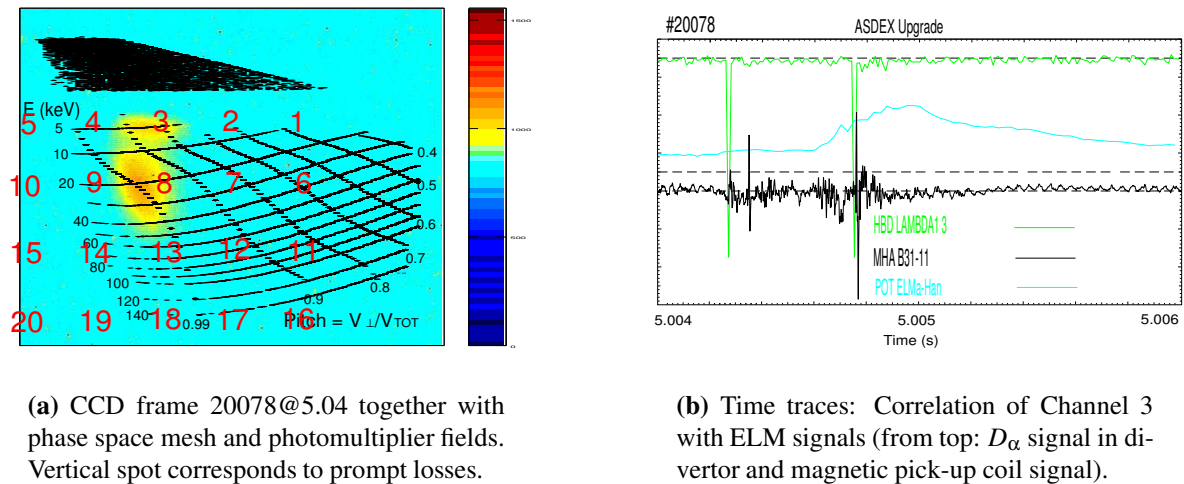


Figure 4: (3,2) NTM induced fast ion losses.

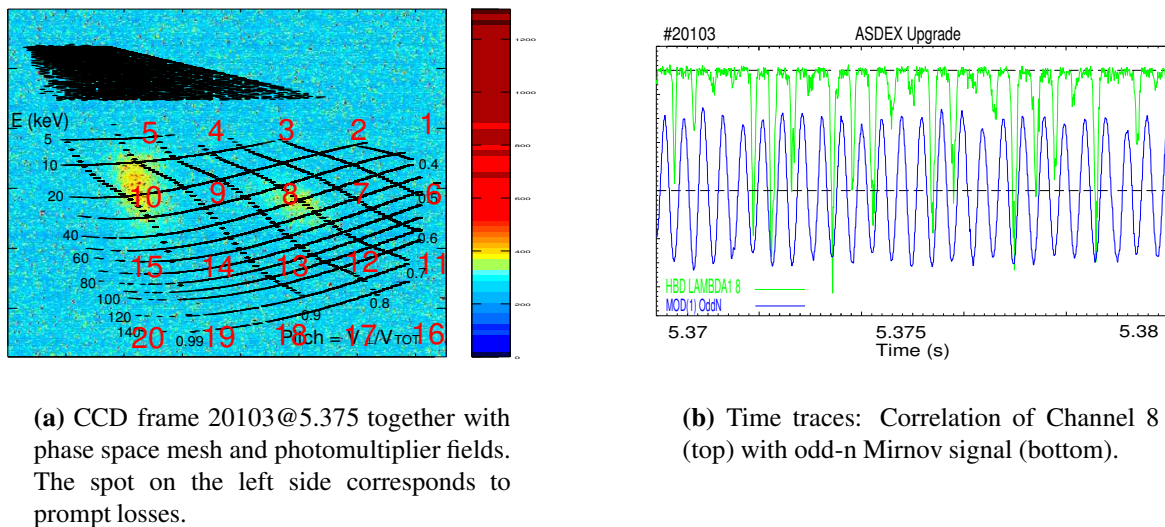


Figure 5: (2,1) NTM induced fast ion losses.

References

- [1] M.Garcia-Munoz, IPP report, **II/6** (2003).
- [2] D. Darrow, Rev. Sci. Instrum. **66**, 476 (1995).
- [3] A. Werner *et al*, Rev. Sci. Instrum. **72**, 780 (2001).
- [4] A. Herrmann, This proceeding (2005).
- [5] R.B. White *et al*, Phys. Fluids **26**, 2958 (1983).